

Supporting Information

Fabrication of bimetallic MOF-74 derived materials for high-efficient adsorption of iodine

Wen-Ze Li,^a Fu-Yu Guo,^a Jing Li,^a Xiao-Sa Zhang,^a Yu Liu,^a and Jian Luan^{*a}

^a College of Science, Shenyang University of Chemical Technology, Shenyang, 110142, P. R. China

E-mail: 2010044@stu.neu.edu.cn (J. Luan)

Table S1 Analysis of metal components in bimetallic MOF-74 system and pyrolyzed Mn-Ni-CX samples by ICP-AES.

Samples	Element	Wt.%
Mn-Zn-MOF-74	Mn	12.288
	Zn	10.157
Mn-Co-MOF-74	Mn	9.517
	Co	12.280
Mn-Ni-MOF-74	Mn	8.159
	Ni	12.790
Mn-Ni-C200	Mn	9.541
	Ni	15.279
Mn-Ni-C400	Mn	15.794
	Ni	25.318
Mn-Ni-C600	Mn	20.516
	Ni	33.417

Supporting Information

Table S2 Comparison of adsorption effect of Mn-Ni-C400 and other materials in iodine solution and iodine vapor.

Materials	Adsorbed state of iodine	Adsorption capacity (mg g ⁻¹)	Reference
MOF-5	Solution	155	S1
Cu-MOF	Solution	144	S2
Mn-Ni-C400	Solution	210	This work
Cu-MOF	Vapor	610	S2
Ni-MOF	Vapor	640	S3
Mn-Ni-C400	Vapor	720	This work

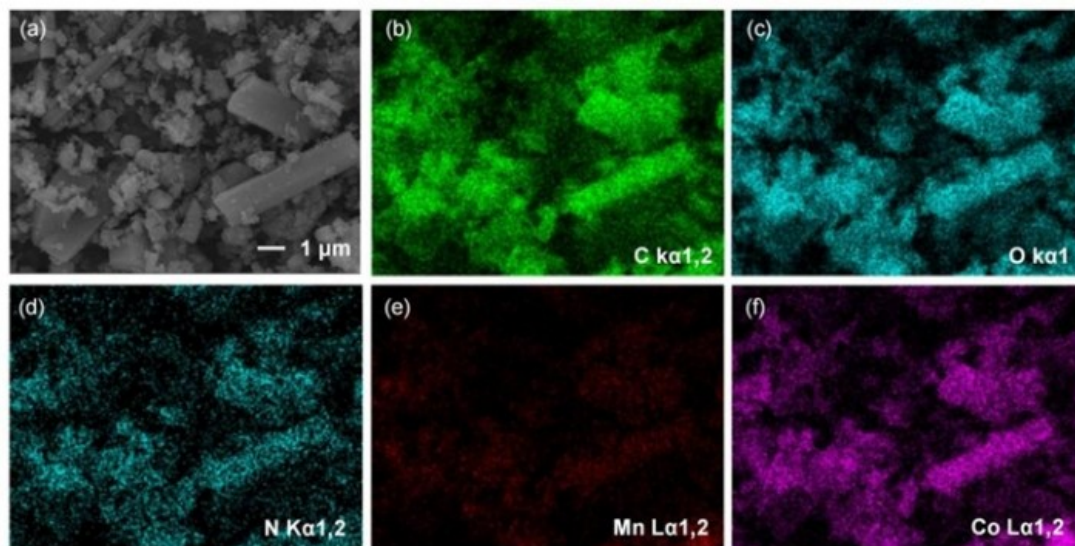


Fig. S1 (a) SEM images of Mn-Co-MOF-74. (b–g) EDX elemental distribution mapping images of Mn-Co-MOF-74.

Supporting Information

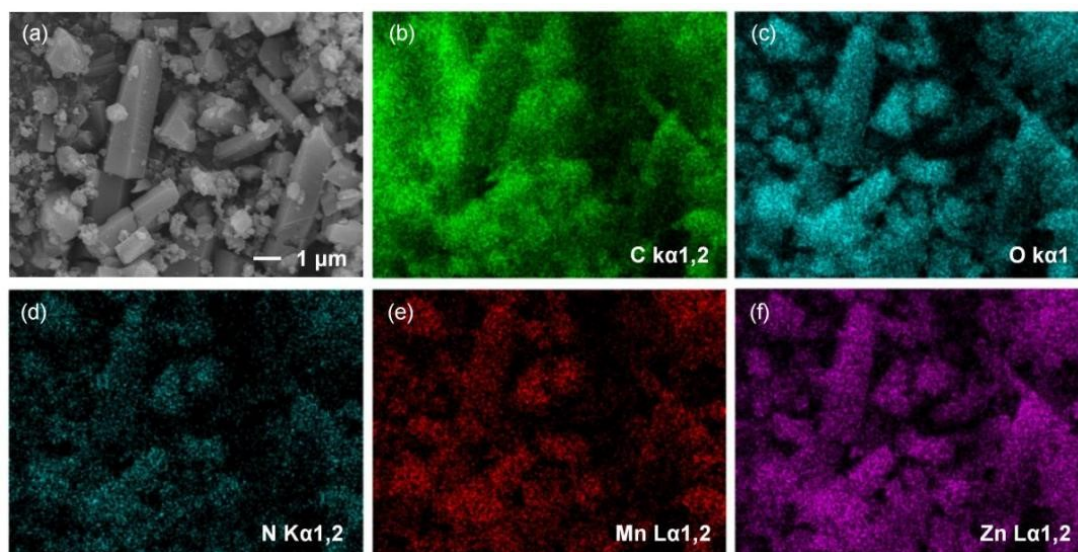


Fig. S2 (a) SEM images of Mn-Zn-MOF-74. (b–g) EDX elemental distribution mapping images of Mn-Zn-MOF-74.

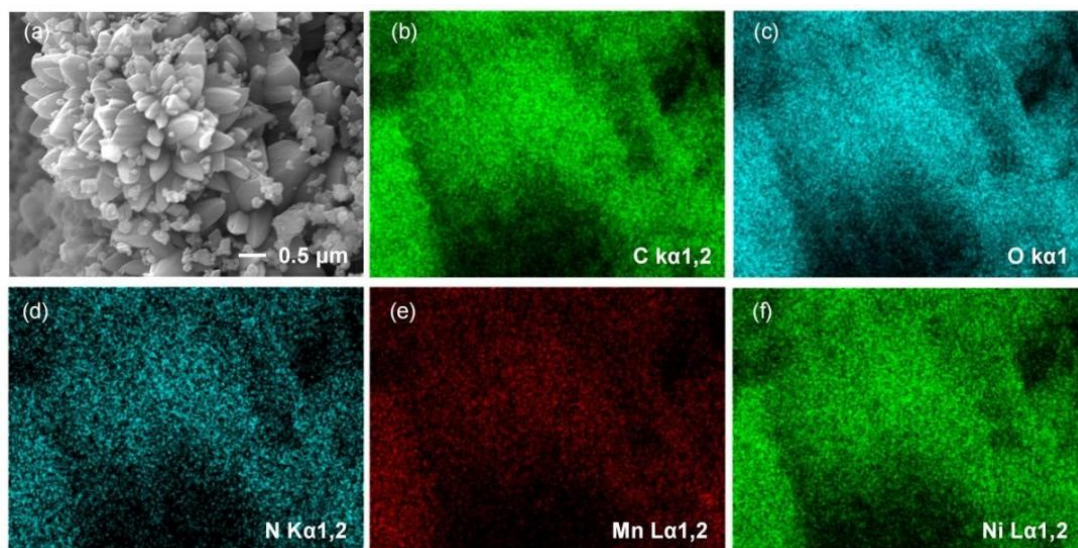


Fig. S3 (a) SEM images of Mn-Ni-C200. (b–g) EDX elemental distribution mapping images of Mn-Ni-C200.

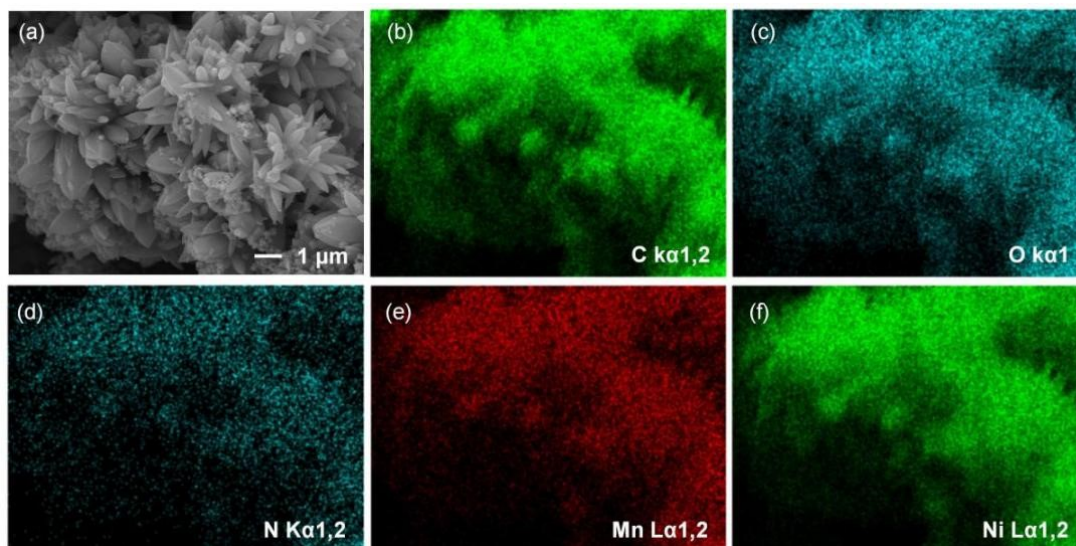


Fig. S4 (a) SEM images of Mn-Ni-C600. (b–g) EDX elemental distribution mapping images of Mn-Ni-C600.

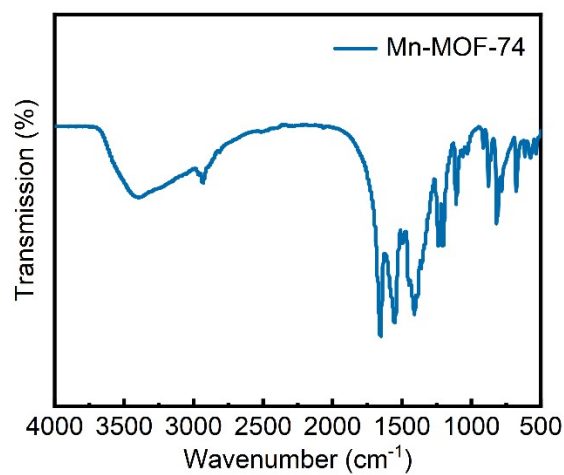


Fig. S5 FTIR spectrum of monometallic Mn-MOF-74.

Supporting Information

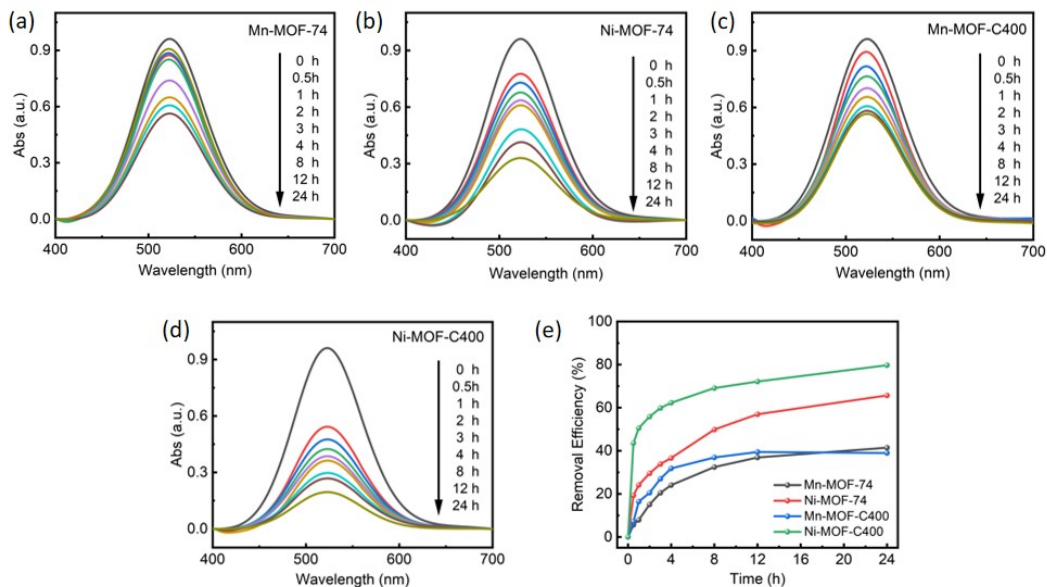


Fig. S6 UV-Vis spectra at different temperatures in iodine-cyclohexane solution at 0.001 mol/L concentration: (a) Mn-MOF-74, (b) Ni-MOF-74, (c) Mn-MOF-C400, (d) Ni-MOF-C400; (e) Removal efficiency.

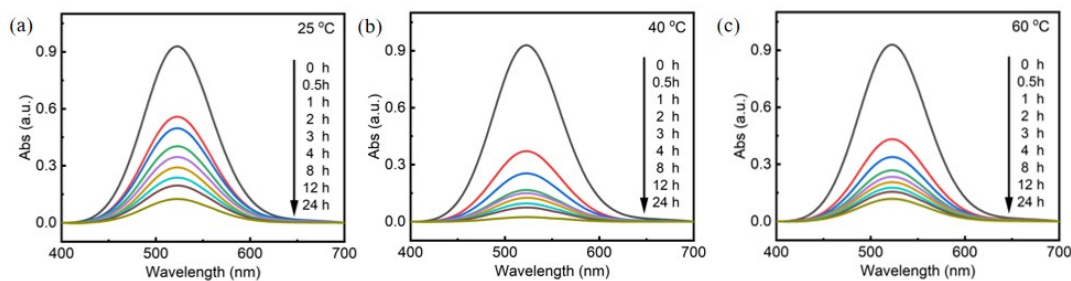


Fig S7 UV-Vis spectra at different temperatures in iodine-cyclohexane solution at 0.001 mol/L concentration: (a) Mn-Ni-C200, (b) Mn-Ni-C400, (c) Mn-Ni-C600.

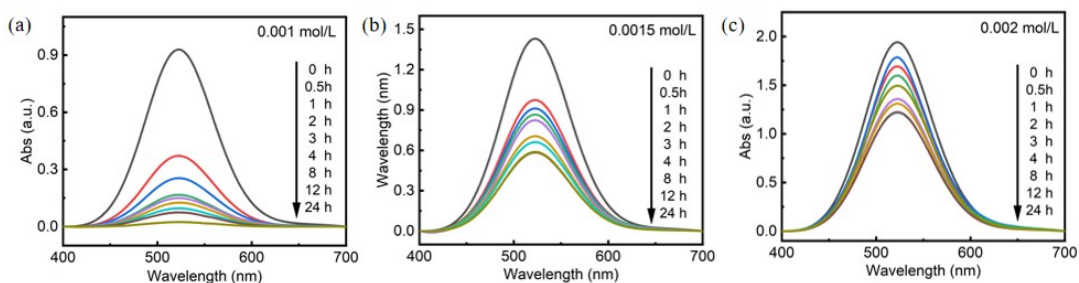


Fig S8 UV-Vis spectra of Mn-Ni-C400 solution with different concentrations of iodine-cyclohexane at 60 °C: (a) 0.001 mol L⁻¹, (b) 0.0015 mol L⁻¹, (c) 0.002 mol L⁻¹.

Supporting Information

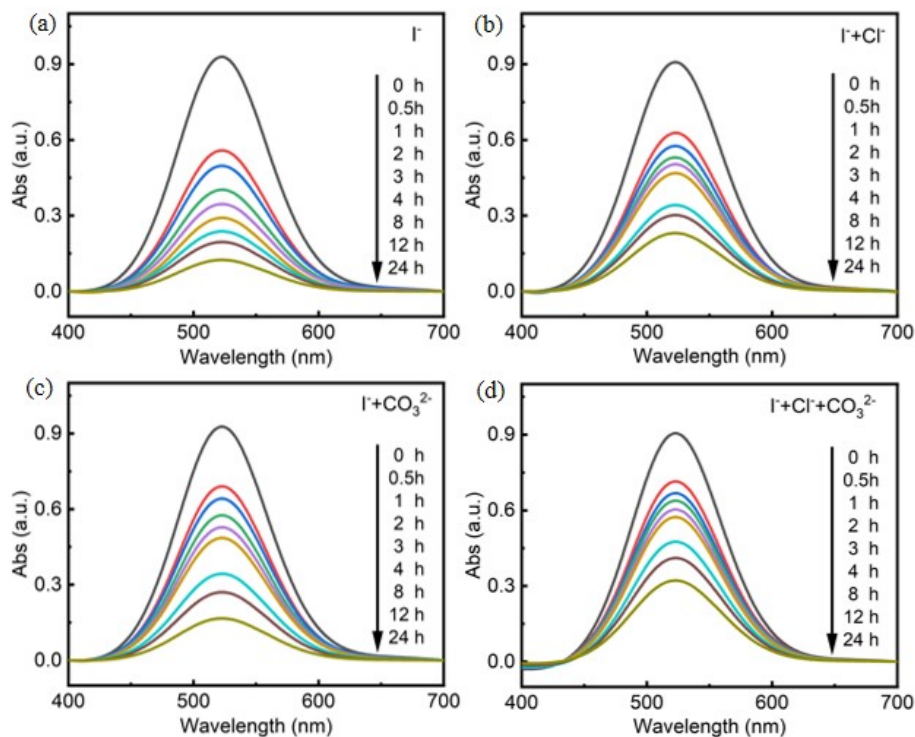


Fig S9 UV-Vis spectra of Mn-Ni-C400 with 0.001 mol L⁻¹ iodine solution added to different interfering ions at 60 °C: (a) I⁻, (b) I⁻ and Cl⁻, (c) I⁻ and CO₃²⁻, (d) I⁻ and Cl⁻ and CO₃²⁻.

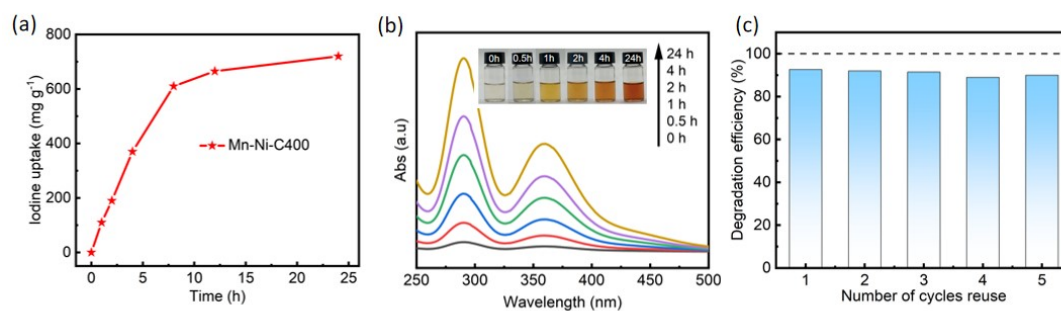


Fig. S10 (a) Iodine vapor experiment of Mn-Ni-C400; (b) The desorption experiment of Mn-Ni-C400@I; (c) Recyclability of Mn-Ni-C400 (after desorption with anhydrous ethanol) for iodine vapor capture.

Supporting Information

Reference:

S1 R. L. Yu, Q. F. Li, T. Zhang, Z. L. Li and L. Z. Xia, *Process Saf. Environ.*, 2023, **174**, 770–777.

S2 M. Li, G. Y. Yuan, Y. Zeng, Y. Y. Yang, J. L. Liao, J. J. Yang and N. Liu, *J. Radioanal. Nucl. Ch.*, 2020, **324**, 1167–1177.

S3 J. Y. Xian, Z. Y. Huang, X. X. Xie, C. J. Lin, X. J. Zhang, H. Y. Song and S. R. Zheng, *Chin. J. Struct. Chem.*, 2023, **42**, 100005.